Electronic Supplementary Information

Boosting Raman Signal on Semiconductor-Nanotube Membrane for Reporting Photocatalytic Reaction on Site

Lingling Yang,[a] Chenxi Zhao,[a] Jingwen Xu,[a] Junli Guo,[a] Zhida Gao,[a] Yan-Yan Song[*a]

[a] College of Sciences, Northeastern University, Shenyang 110004, China

Email: yysong@mail.neu.edu.cn

1. Experimental

1.1 Materials

Ti sheets (0.1 mm thickness, 99.6 % purity) were supplied by Baosheng Hardware Co. Ltd (Bao ji, China). Ammonium fluoride (NH_4F), ethylene glycol, lactic acid (LA), hydrofluoric acid, methanol, ethylenediaminetetraacetic acid (EDTA), p-benzoquinone (BQ), and $K_2Cr_2O_7$ were purchased from Sinopharm Chemical Reagent Co. Ltd. Phosphoric acid (H_3PO_4) and 4-NBT were purchased from sigma.

1.2 Characterization

SERS measurements were conducted using a Raman microscopy spectrometer (LabRAM HR, HORIBA Scientific, France). Ion current was measured using a Keithley 6487 picoammeter (Keithley Instruments, Cleveland, OH). Morphological characterization was carried out using a field-emission scanning electron microscope (FESEM SU 8000, Japan). X-ray photoelectron spectra were recorded using a Perkin–Elmer Physical Electronics 5600 spectrometer using Al Kα radiation at 13 kV as the excitation source. XRD patterns were acquired using an X'Pert XRD spectrometer (Philips, USA) using a CuKα X-ray source. UV-visible diffuse reflectance spectra were obtained using a Perkin-Elmer spectrometer (Lambda 750S, USA). Zeta potentials of NPs were measured using a nano zetasizer (Nano zs90 Malvin Instruments). Contact angle was measured using a Contact angle measuring instrument (HARKE-SPCA).

1.3 Fabrication of sS-TiNM, dS-TiNM, Ref-TiNM-1, and Ref-TiNM-2

The Ti foils (15 mm× 20 mm ×0.125 mm) were anodized in a hot H_3PO_4/HF electrolyte (100 °C). Anodization experiments were carried out at 15 V for 2 h. After anodization, the anodized samples were immersed in ethanol overnight and dried under N_2 stream. Then, the samples were annealed at 150 °C in air for 1 h to remove the residual F^- from the electrolyte.[1] This heating treatment ensured that the first layer of nanotubes will not be damaged during the second anodization. The second anodization was carried out from ethylene electrolyte containing 0.1 M NH_4F and 1.5 M LA at 120 V for 14 min. The titanium substrate was then removed by H_2O_2 (30%) to obtain a free-standing smooth TiO_2 nanotube-based membrane (dS-TiNM).

For reference TiNM-1 (Ref-TiNM-1), the Ti sheet was anodized at 120 V for 14 min in an ethylene glycol-based electrolyte containing 0.1 M NH_4F and 1.5 M LA. The as-formed nanotube layers were removed by ultrasonication, and a second anodization was carried out under the same experimental conditions as those used for the first step. For reference TiNM-2 (Ref-TiNM-2), the

anodization conditions are the same as TiNM-1 and without second anodization.

1.4 Deposition of AuNPs

To form Au nanoparticles (AuNPs) on the sample, a plasma-sputtering machine (EM SCD 500, Leica) was used to sputter-coat Au thin films. The applied sputtering current was 15 mA, and the pressure of sputtering chamber was set at 10^{-2} mbar of Ar. The amount of sputtered material was *in situ* determined using an automated quartz crystal monitor and is reported in this study as the nominal thickness of sputtered film. The Au film sputtered on sample without further treatment. And the sputtering thickness was controlled based on automated quartz crystal monitor on the sputtering machine.

1.5 photocatalytic experiment

A LED light with the main emission at 365 nm was used as the exciting light. The power of LED was monitored using a dynamometer (OPHIR, NOVA II). The power of LED was controlled by adjust the distance of the sample and LED light. The Au/dS-TiNM substrate was first immersed in 4-NBT (10^{-3} M) solution overnight. Then, the sample was rinsed with deionized (DI) water for three times and then dried at room temperature. Before photocatalytic experiments, 10 μL DI water was dropped on sample surface to keep the sample surface moist, and then, LED light irradiated the sample for different period. The LED light was fixed on the Raman operating table, and SERS spectra were immediately collected after the LED light switched off.

1.6 SERS analysis

SERS spectra of the samples were measured using a Raman microscope (LabRAM HR, HORIBA Scientific, France) with a 50× objective using an excitation wavelength of 638 nm with a laser intensity of 13.8 mW/cm². The acquisition time was 5 s; the confocal hole size was 500 μm; the slit aperture size was 200 μm.

1.7 Electrochemical measurement

The Au/dS-TiNM was mounted between two halves of a conductivity cell, and each half-cell was filled with 1 μM KCl solution. Current was measured using a Keithley 6487 picoammeter voltage source (Keithley Instruments). A pair of homemade Ag/AgCl electrodes were set in each half-cell to apply the desired transmembrane potential and to measure the resulting ionic current. The main transmembrane potential used in this study had a scanning voltage from –1 V to +1 V with a rate of 400 mV/s.

1.8 Photocurrent measurement

The photoelectrochemical properties of different AuNP-decorated dS-TiNMs were evaluated using a classical three-electrode setup in 0.1 M Na_2SO_4. The AuNP-decorated dS-TiNM acted as the working electrode; a platinum plate acted as the counter electrode; a Ag/AgCl (3 M KCl) electrode acted as the reference electrode. The applied bias was +0.5 V. The light source was the LED light

2. Supplementary Figures

SEM images
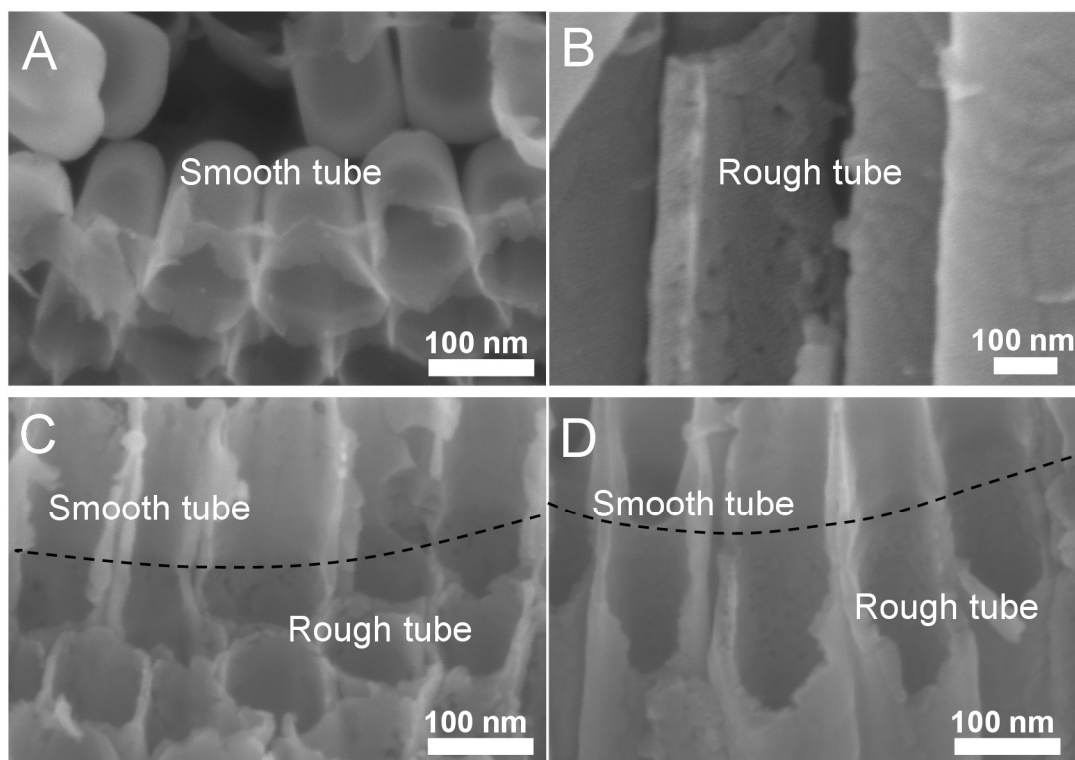
Fig. S1 The SEM cross-section view of (A) smooth tubes and (B) rough tubes; (C-D) the SEM cross-section view of dS-TiNM.

XRD patterns
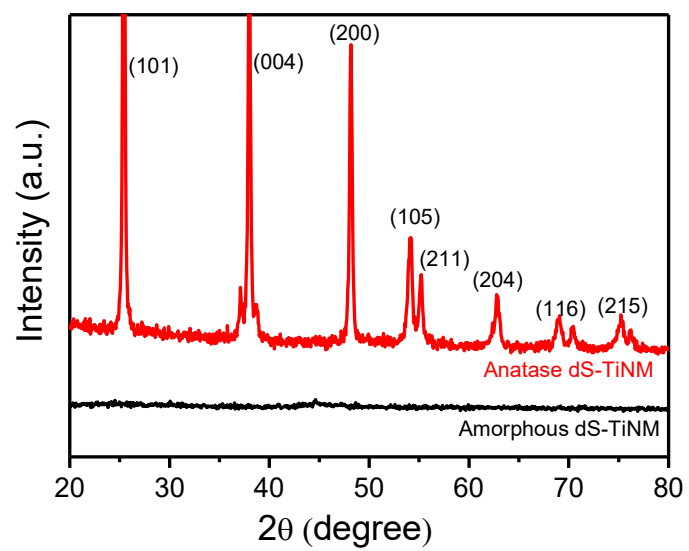
Fig. S2 XRD patterns of amorphous dS-TiNM, anatase dS-TiNM.

Optimized AuNPs
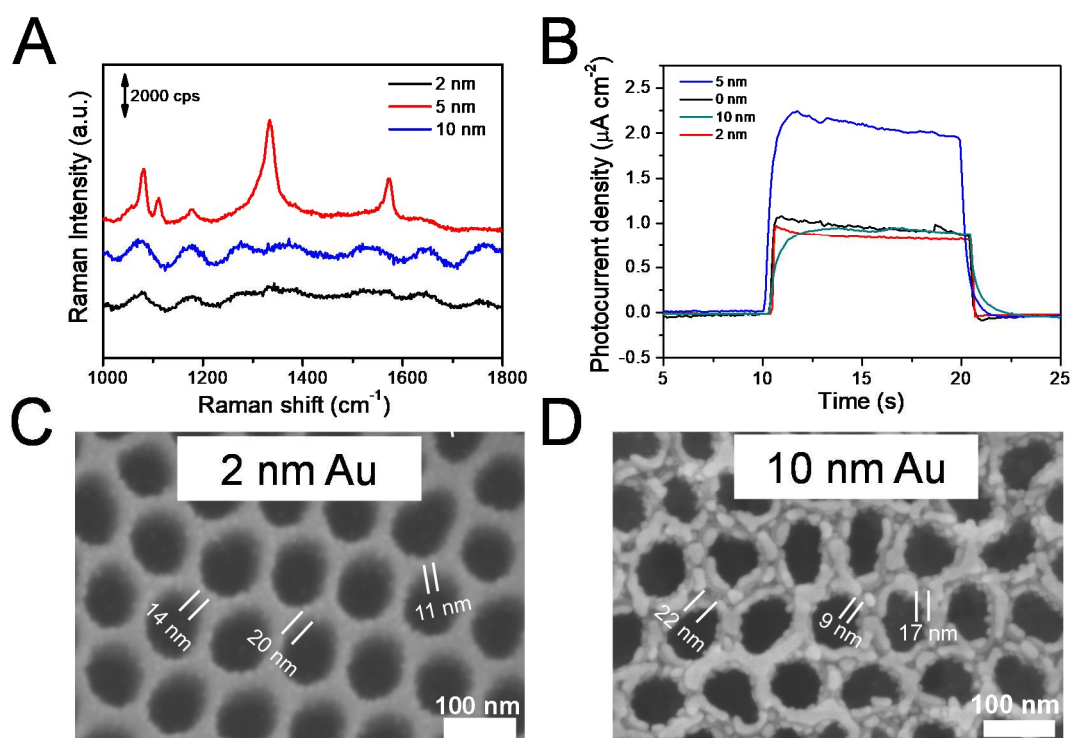
Fig. S3 (A) Raman spectra of 10^{-3} M 4-NBT absorbed on Au/dS-TiNM with different sizes of AuNP sputtering. (B) Photocurrents of dS-TiNM and dS-TiNM decorated with 2 nm, 5 nm, and 10 nm AuNPs. (C) SEM images of 2 nm AuNP decorated dS-TiNM, (D) 10 nm AuNP decorated dS-TiNM.

The "hot spot" is reported to the major factor that influences the SERS activity. For the electromagnetic enhancement, the enhancement of Raman signals are caused by the high electromagnetic fields that exist in the small gaps between metal nanostructures, which are called hot spots.[2] To form plenty "hot spots", the absorbance band of Au NPs should match the exciting light, and the optimized size of gaps for the formation of "hot spots" is reported as 1-5 nm.[3] In our case, the poor Raman activities of 2-nm and 10-nm Au decorated samples could be contributed to the larger gap size between Au NPs. As shown in the SEM images in Fig. S3C and D, it can be seen that the gap size for 2-nm and 10-nm Au decorated samples are 11-20 nm and 9 -22 nm, respectively.

In our system, Au NPs act as the co-catalysts to improve the photocatalytic activity of TiO_2.[4] The photocatalytic activity of Au/TiO_2 hybrid could be attributed to the prevailing effect of shape and size dependent co-catalytic activity of AuNPs imparted to TiO_2. For 2-nm AuNPs, rather than accelerating charge transport and reducing the charge recombination, these AuNPs may act as the electron–hole recombination center and reduce the quantum efficiency.[4] For 10-nm AuNPs, the drop in the photocatalytic activity probably originates from the largely covered TiO_2 surface by Au NPs. Furthermore, the larger Au NPs also act as recombination centers for electron–hole pairs.[5,6] Therefore, the size of cocatalyst is one of important factors to influence the photoactivity of TiO_2.

EF calculation
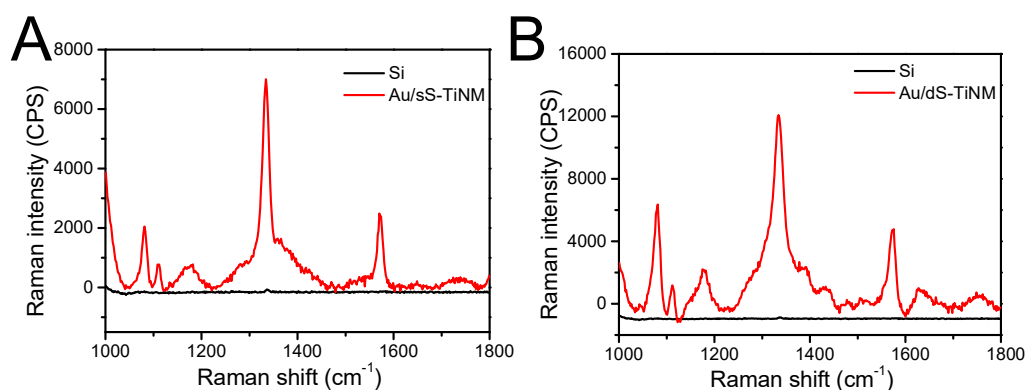
Fig. S4 (A) SERS spectra of 10^{-5} M 4-NBT adsorbed on Au/sS-TiNM, and SERS spectra of 5×10^{-3} M 4-NBT adsorbed on Si slide. (B) SERS spectra of 10^{-3} M 4-NBT adsorbed on Au/dS-TiNM, and SERS spectra of 5×10^{-3} M 4-NBT adsorbed on Si slide.

To calculate the EF of Au/sS-TiNM and Au/dS-TiNM, 5 μL of 10^{-5} 4-NBT solution and 5 μL of 10^{-3} M 4-NBT solution were dropped and spread on the Au/TiNM substrate (5 mm × 5 mm scale) and Au/dS-TiNM substrate (5 mm × 5 mm scale), respectively. As a non-SERS sample, 50 μL of 5×10^{-3} M 4-NBT aqueous solution was dropped and spread on a Si slide and dried at room temperature. The Raman spectra were recorded using 638 nm wavelength lasers (100% power) with 50× objective, and data acquisition time was kept at 5 s.

The EF was evaluated using the following eq:[7,8]

$$EF = \frac{I_{SERS}/N_{SERS}}{I_0/N_0} \tag{1}$$

$$N = CVN_AS_{sub} \tag{2}$$

where N_0 and N_{SERS} are the corresponding number of 4-NBT molecules on non-SERS and SERS substrate, respectively. The number of probe molecules was estimated using Eq 2, where N_A is Avogadro constant, C is the molar concentration of the probe solution, V is the volume of droplet, and S_{sub} is the area of substrate. The Raman spectra of 4-NBT on SERS and non-SERS substrates are shown in Fig. S3B. According to Eqs. 1 and 2, the EFs on a single-layered sS-TiNM and two-layered dS-TiNM were calculated as 5.0×10^6 and 1.4×10^4, respectively.

UV-vis absorbance spectra
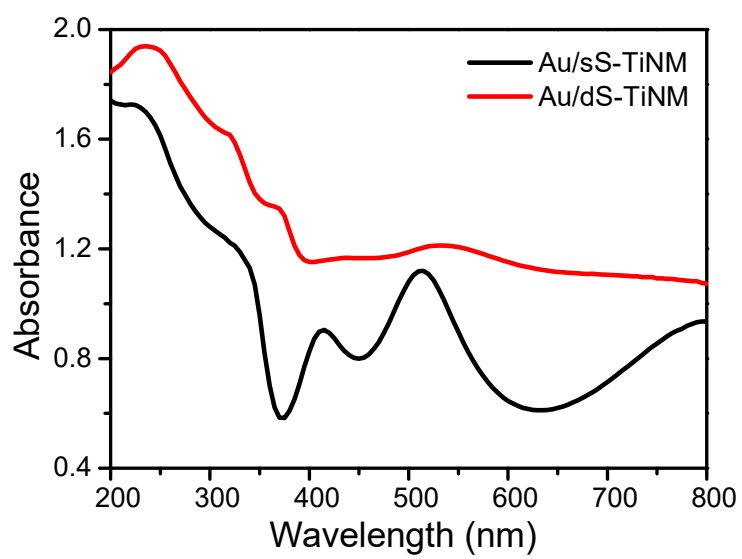
Fig. S5 UV-vis absorbance spectra of Au/sS-TiNM and Au/dS-TiNM.

SERS spectra at different exciting wavelengths
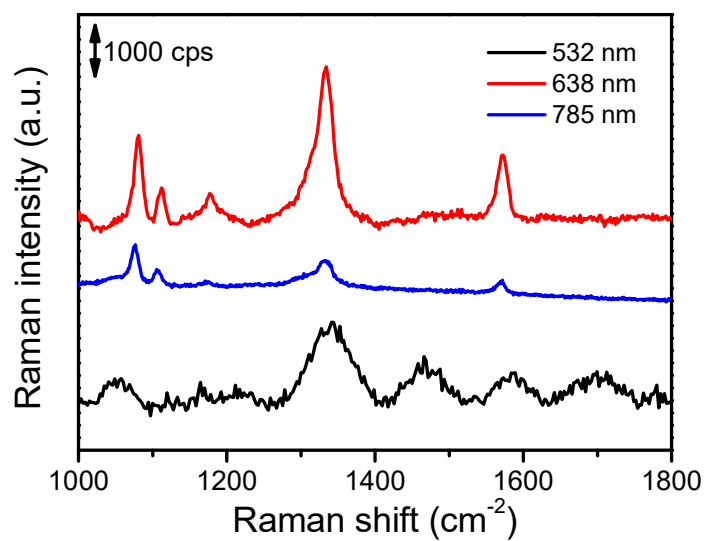
Fig. S6. SERS signal obtained from the same spot on Au/dS-TiNM using 532-nm, 638-nm, and 768-nm lasers as the exciting light source.

SEM images of Ref-TiNM-1 and Ref-TiNM-2
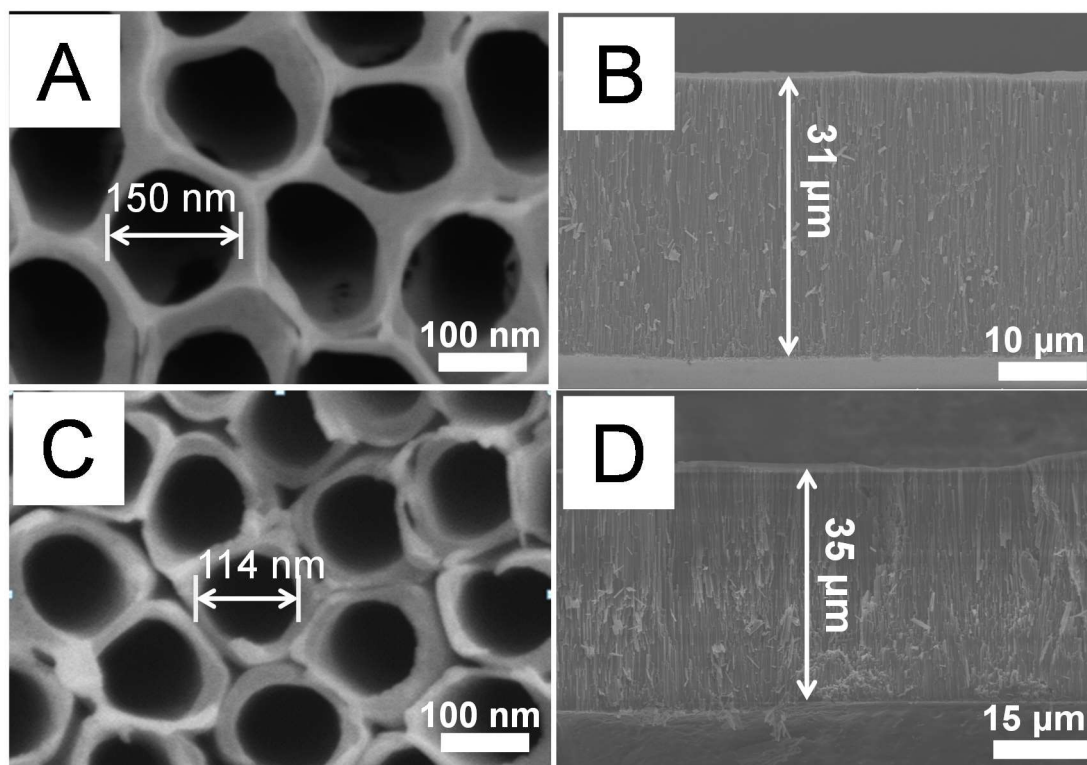
Fig. S7. SEM images: Ref-TiNM-1 (A) top view and (B) side view; Ref-TiNM-2 (C) top view and (D) side view.

Au/Ref-TiNM-1 and Au/Ref-TiNM-2
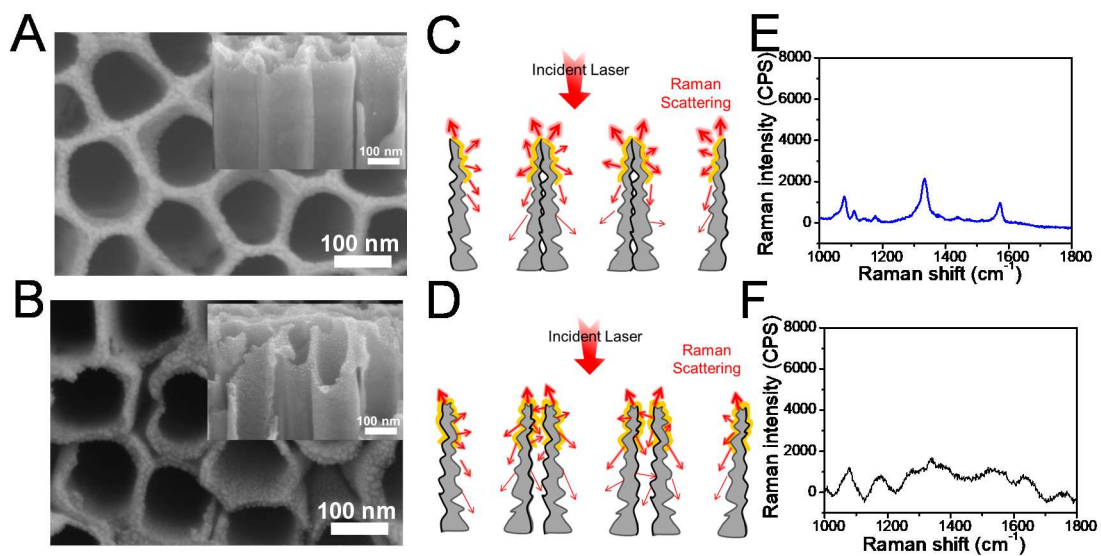
Fig. S8. SEM images of (A) Au/Ref-TiNM-1 and (B) Au/Ref-TiNM-2. Schematic diagram of light absorption and refraction mechanism of (C) Au/Ref-TiNM-1 and (D) Au/Ref-TiNM-2. Raman spectra of 10^{-3} M 4-NBT absorbed on (E) Au/Ref-TiNM-1 and (F) Au/Ref-TiNM-2.

UV-vis absorbance spectra and UV-vis reflectance spectra
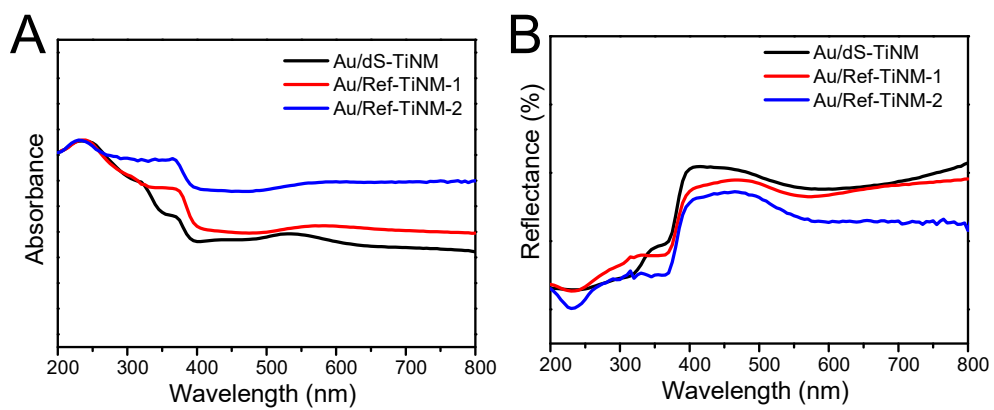
Fig. S9. (A) UV-vis absorbance spectra and (B) UV-vis reflectance spectra of Au/dS-TiNM, Au/Ref-TiNM-1, and Au/Ref-TiNM-2.

SERS spectra
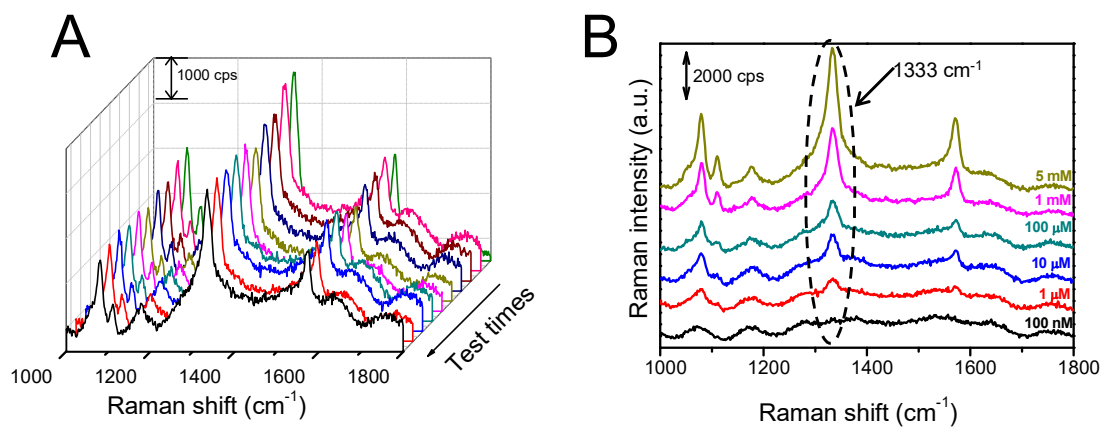
Fig. S10. (A) SERS spectra of 10^{-3} M 4-NBT collected from 10 randomly selected positions on Au/dS-TiNM. (B) SERS spectra of different concentrations of 4-NBT absorbed on Au/dS-TiNM.

Sensing and Photocatalytic mechanism
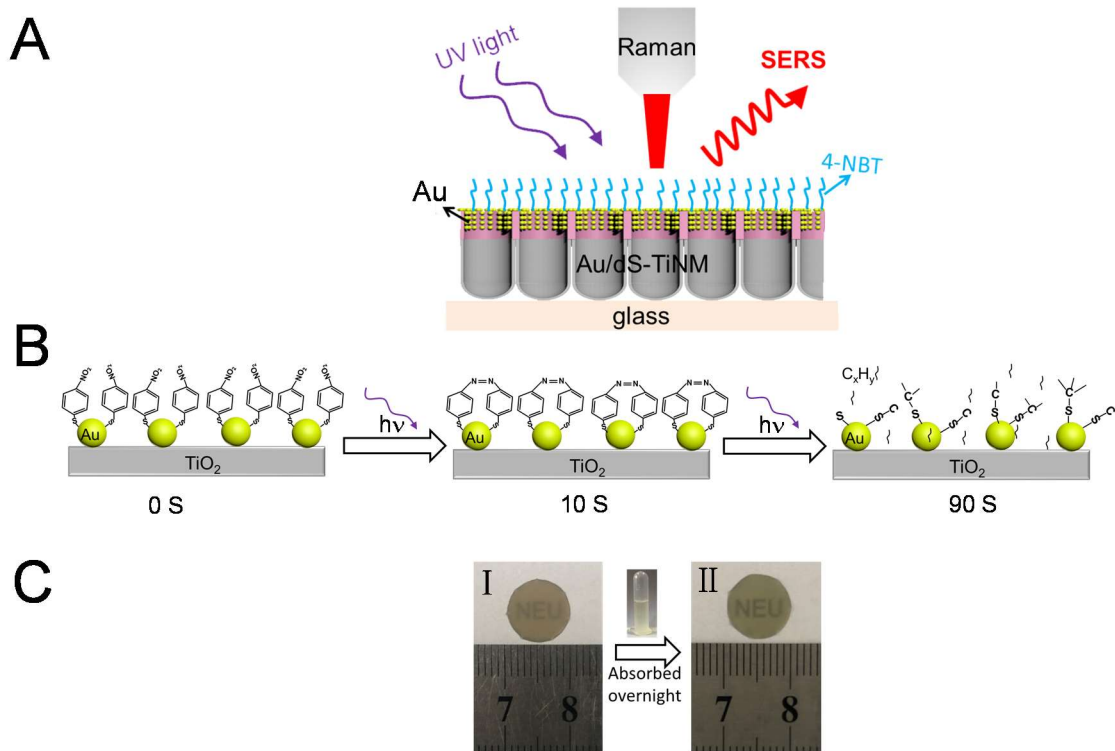
Fig. S11 (A) The schematic setup for the detection of 4-NBT and DMAB on Au-TiNM *via* SERS technique. (B) The schematic machemism of photocatalytic processes on Au/dS-TiNM. (C) The digital photographs of Au/dS-TiNM before (I) and after (II) 4-NBT absorption.

XPS patterns
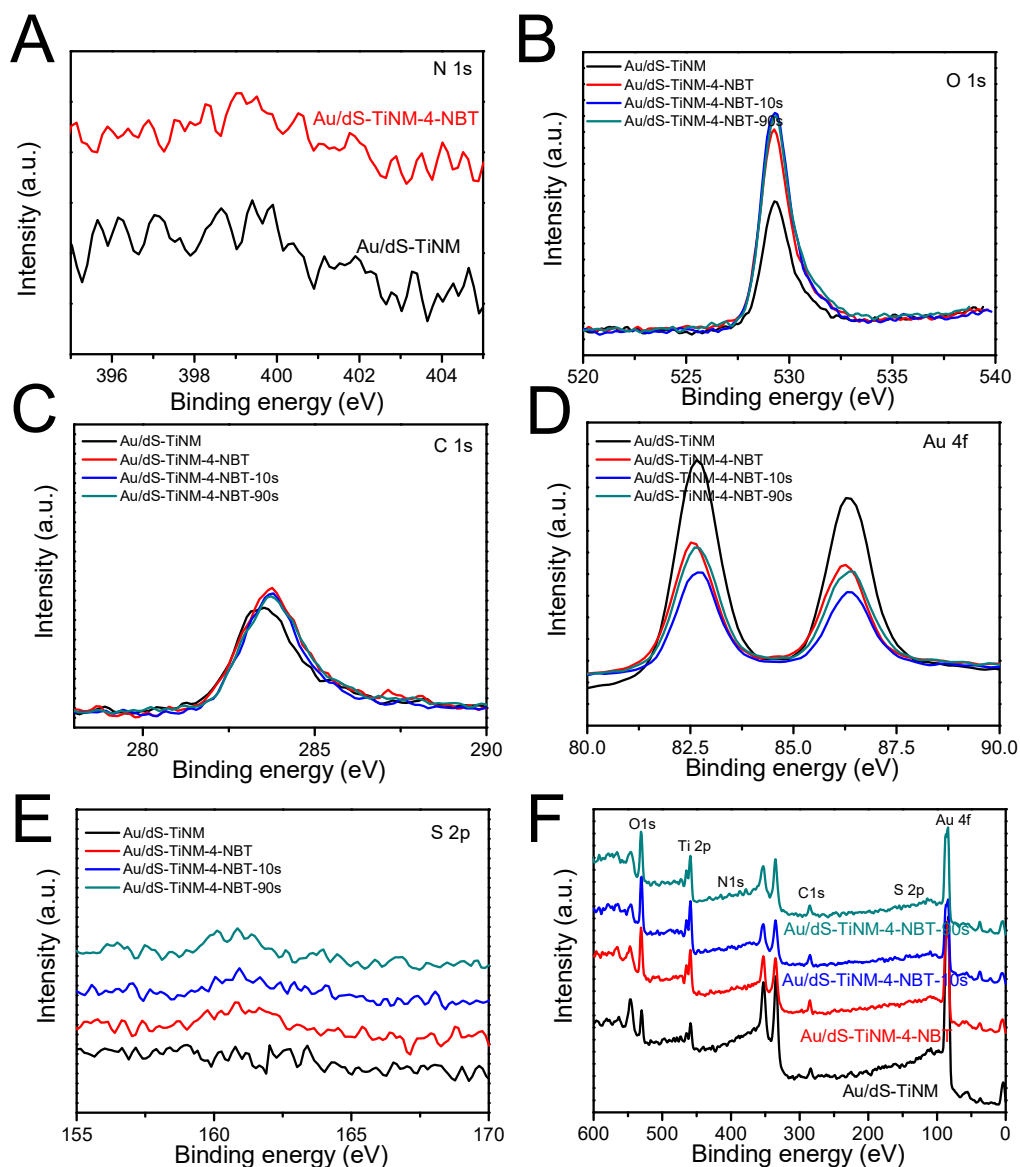
Fig. S12. High-resolution XPS spectra of (A) N 1s, (B) O 1s, (C) C 1s, (D) Au 4f, and (E) S 2P. (F) XPS survey spectra of Au/dS-TiNM, Au/dS-TiNM-4-NBT-0 s, Au/dS-TiNM -4-NBT-10 s, and Au/dS-TiNM -4-NBT-90 s.

Changes of contact angle on 4-NBT absorbed Au/sS-TiNM
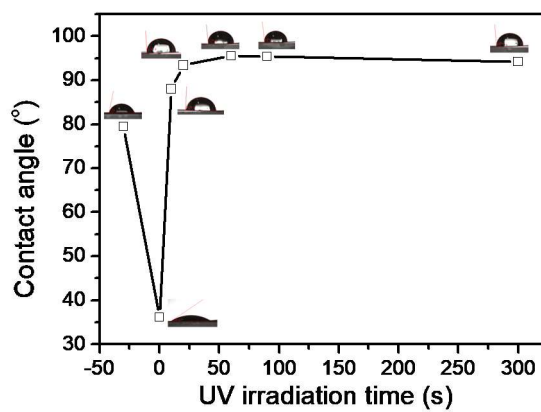
Fig. S13. Changes in contact angle on 4-NBT absorbed Au/sS-TiNM under LED irradiation (365 nm, 30 mW cm^{-2}) for different times.

Changes in Zeta potential of Au/dS-TiNM-4-NBT under LED irradiation
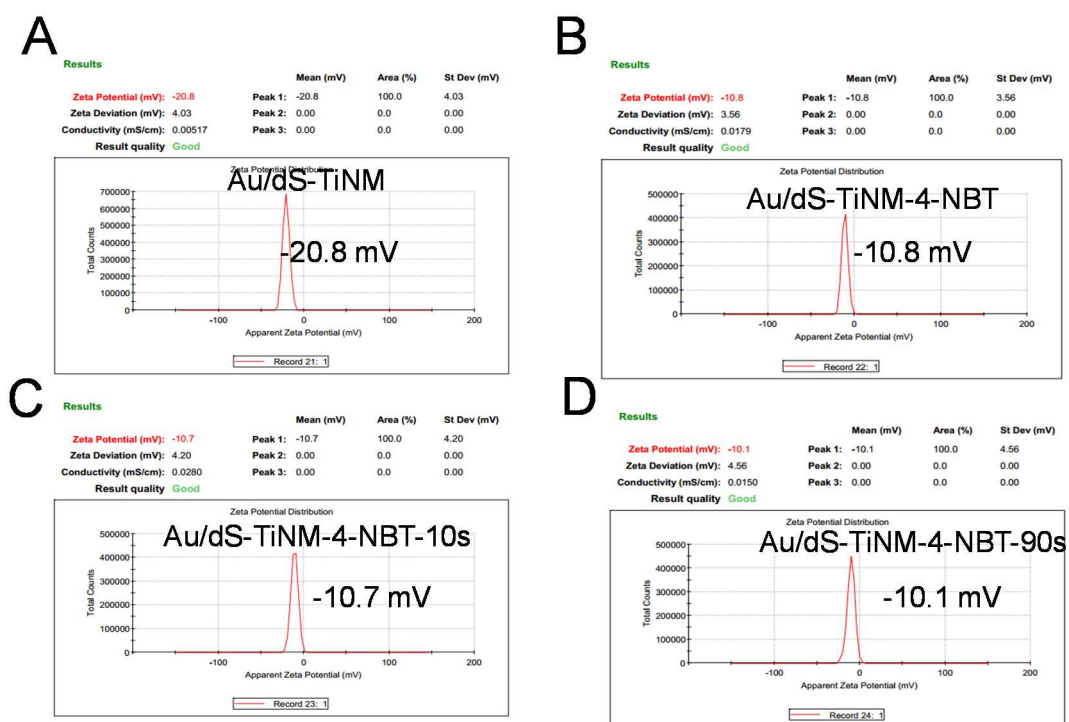
Fig. S14. Zeta potential of (A) Au/dS-TiNM and 4-NBT absorbed Au/dS-TiNM after irradiating with LED for (B) 0 s, (C) 10 s, and (D) 90 s.

Schematic diagram of real-time transmembrane current measurement
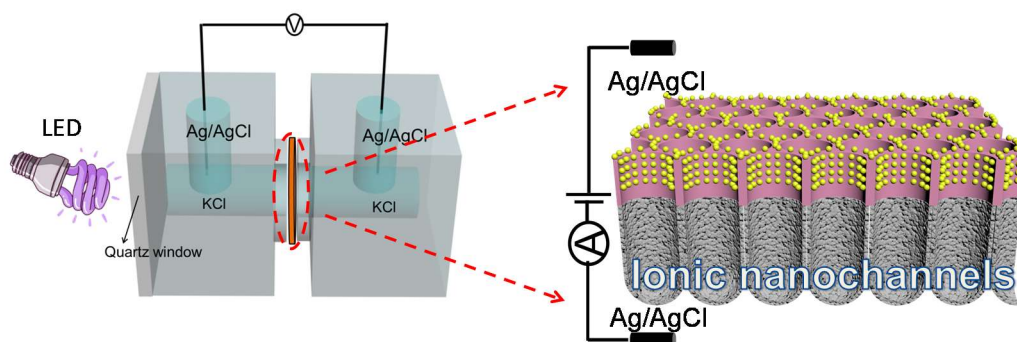
Fig. S15. Schematic diagram of real-time transmembrane current measurement under LED irradiation.

_I–V_ curves for Au/dS-TiNM
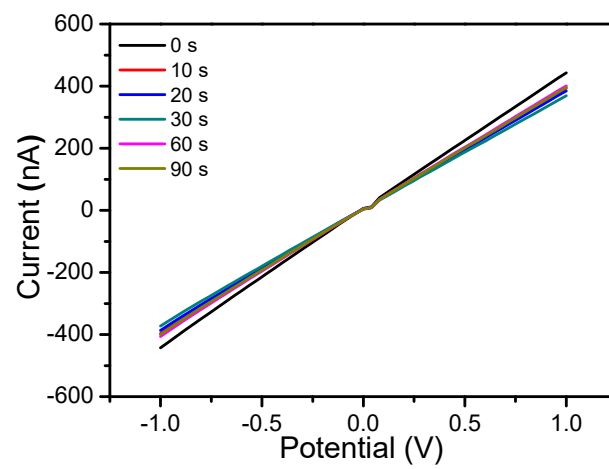
Fig. S16. Real-time _I–V_ curves for Au/dS-TiNM illuminated by LED irradiation for different times.
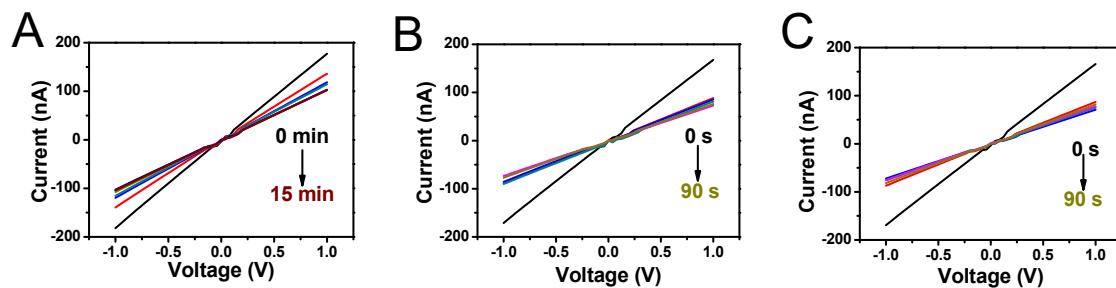
Fig. S17. Real-time *I−V* curves recorded for 4-NBT-modified Au/dS-TiNM under LED irradiation. (A: 10 mW cm^{-2}; B: 30 mW cm^{-2}; C,: 60 mW cm^{-2})

Reference

(1) S. So, I. Hwang, J. E. Yoo, S. Mohajernia, M. Macˇkovic´, E.n Spiecker, G. Cha, A. Mazare and P. Schmuki *Adv. Energy Mater.* 2018, **8**, 1800981.

(2) E.-Z. Tan, P.-G. Yin, T. You, H. Wang and L. Guo *ACS Appl. Mater. Interfaces* 2012, **4**, 3432.

(3) S. Y. Ding, E. M. You, Z. Q. Tian and M. Moskovits, Chem. Soc. Rev., 2017, **46**, 4042.

(4) K. Rupinder and P. Bonamali *J. Mol. Catal. A: Chem.* 2012, **355**, 39.

(5) M. Murdoch, G. I. N. Waterhouse, M. A. Nadeem, J. B. Metson, M. A. Keane, R. F. Howe, J. Llorca and H. Idriss *Nat. Chem.* 2011, **3**, 489.

(6) C. Feng, Z. Yu, H. Liu, K. Yuan, X. Wang, L. Zhu, G. Zhang and D. Xu *Appl. Phys. A* 2017, **123**, 519.

(7) S. Lal, N. K. Grady, G. P. Goodrich and N. J. Halas, *Nano Lett.* 2006, **6**, 2338.

(8) E. C. Le Ru, E. Blackie, M. Meyer and P. G. Etchegoin *J. Phys. Chem. C* 2007, **111**, 13794.